

A hybrid BIE-WOS (Boundary Integral  
Equation-Random Walk on Spheres)  
Method for Laplace Equations

Wei Cai

Dept. of Math & Stat. UNC Charlotte

**NIST**  
**2015-4-15**

## Outline

- Domain Decomposition Boundary Integral Equation
- Probabilistic solution for Dirichlet and Neumann data
- Numerical Results & Scaling performance
- Summary & open issues

## How to get best parts of two worlds?

- Finite Element/Difference: local method, but ill-conditioned
- Integral equation method: well-conditioned, but global method
- Our goal: Produce a local well conditioned integral equation method by introducing Stochastic techniques -  
i.e. Feynman-Kac formula

- **Previous work using WOS MC for PB equ.**
- J. A. Given, C. O. Hwang, and M. Mascagni, First-and last-passage Monte Carlo algorithms for the charge density distribution on a conducting surface, *Phys. Rev. E*, 66 (2002), 056704.
- M. Mascagni and N. A. Simonov (2004), "Monte Carlo Methods for Calculating Some Physical Properties of Large Molecules," *SIAM Journal on Scientific Computing*
- T. Mackoy, R. C. Harris, J. Johnson, M. Mascagni and M. O. Fenley (2013), "Numerical Optimization of a Walk-on-Spheres Solver for the Linear Poisson-Boltzmann Equation," *Communications in Computational Physics*, 13: 195-206.

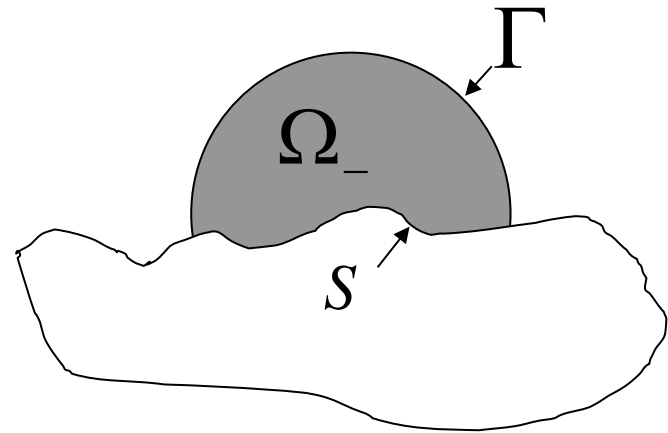
- **Publication**

C.H. Yan, W. Cai, X. Zeng, A parallel method for solving Laplace equations with Dirichlet data using local boundary integral equations and random walks. **SIAM J. Scientific computing** (2013), vol. 35, No. 4, pp. B868-B889.

# DD Boundary Integral Equation

$$-\Delta u(x) = 0, x \in \Omega$$

$$u|_{\partial\Omega} = f, \text{ or } \frac{\partial u}{\partial n}|_{\partial\Omega} = f$$



$$-\Delta G(x, y) = \delta(x - y), x, y \in \Omega_- \quad G|_{\Gamma} = 0$$

$$u(x) = \int_{\Gamma} \frac{\partial G}{\partial n} u(y) ds_y + \int_S \left[ \frac{\partial G}{\partial n} u(y) + G \frac{\partial u}{\partial n} \right] ds_y$$

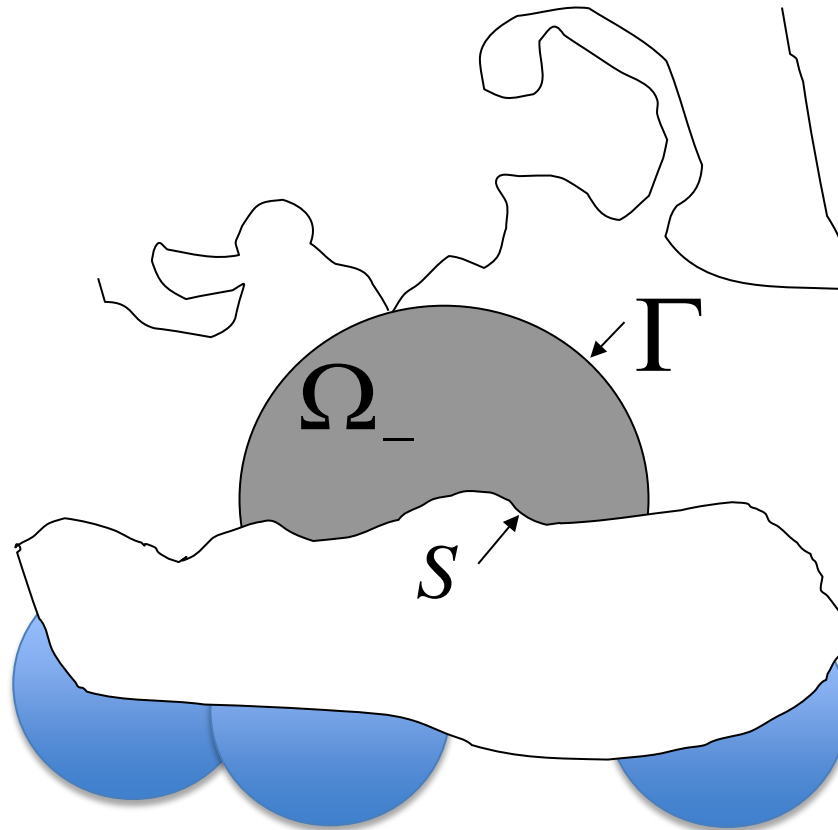
$$\frac{1}{2} \frac{\partial u}{\partial n_x} = \int_{\Gamma} \frac{\partial^2 G}{\partial n_y \partial n_x} u(y) ds_y + p.f. \int_S \left[ \frac{\partial^2 G}{\partial n_y \partial n_x} u(y) + \frac{\partial G}{\partial n_x} \frac{\partial u}{\partial n_y} \right] ds_y$$

$$x \in S$$

$$\left( \frac{1}{2} I + K \right) \frac{\partial u}{\partial n} = f$$

2<sup>nd</sup> kind integral equations

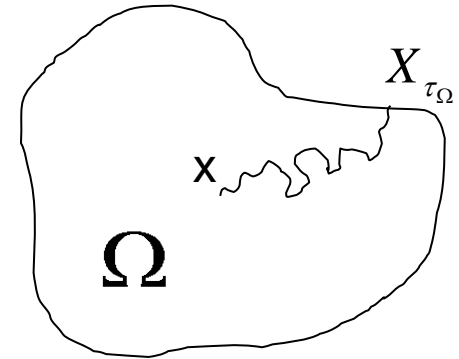
# Domain Decomposition Boundary Element Methods



# Feynman-Kac formula (Dirichlet Problem)

$X_t(\omega)$  a stochastic process of Ito diffusion

$$dX_t = b(X_t)dt + \sigma(X_t)dB_t$$



The solution to the following elliptic PDE

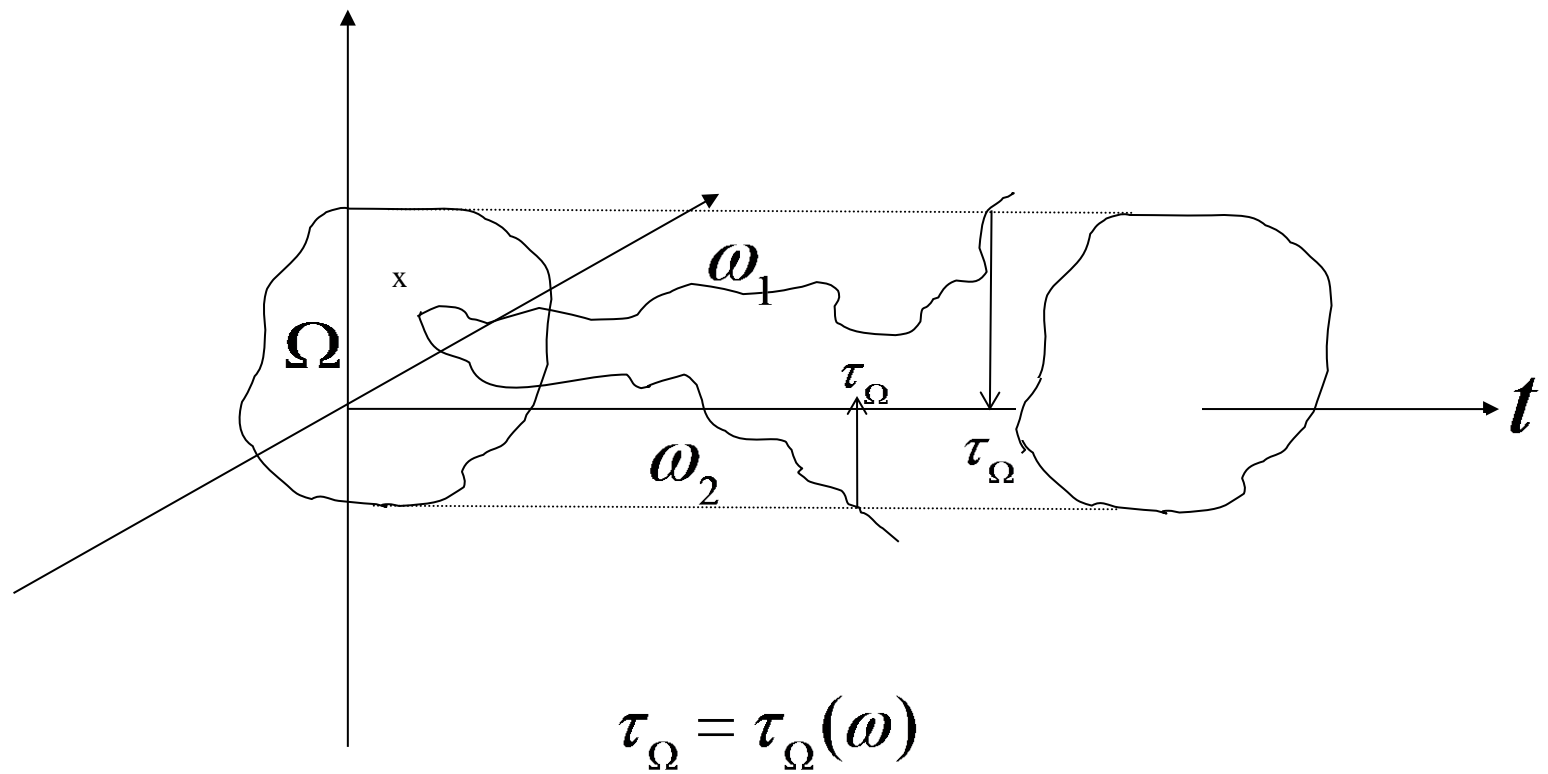
$$Lu(x) = -g \quad u|_{\partial\Omega} = \phi(z), z \in \partial\Omega$$

$$L = \sum_{i=1}^n b_i(x) \frac{\partial}{\partial x_i} + \sum_{i,j=1}^n a_{ij}(x) \frac{\partial^2}{\partial x_i \partial x_j} \quad [a_{ij}] = \frac{1}{2} \sigma(x) \sigma^T(x)$$

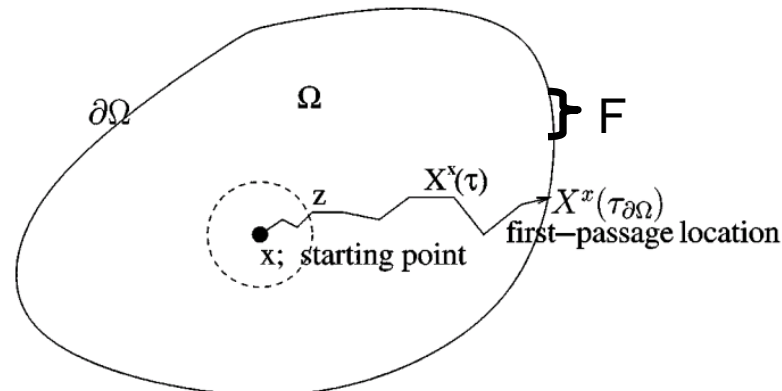
$$u(x) = E^x[\phi(X_{\tau_\Omega})] + E^x\left[\int_0^{\tau_\Omega} g(X_t)dt\right]$$

$\tau_\Omega$  Exit time

$\tau_{\Omega}$  Exit time (first passage)



# Exit (first passage) time and Harmonic measure



$$u(x) = E^x[\phi(X_{\tau_\Omega})] = \int_{\partial\Omega} \phi(y) d\mu_\Omega^x$$

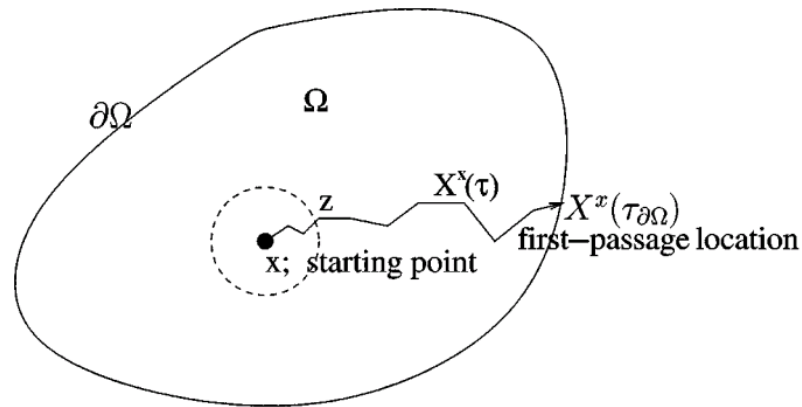
Harmonic measure on the boundary

$$\mu_\Omega^x(F) = P^x\{\omega \mid X_{\tau_\Omega}(\omega) \in F, X_0(\omega) = x\}, F \subset \partial\Omega, x \in \Omega$$

For a ball centered at  $x$

$$\mu_\Omega^x(F) \approx ds_y$$

# Green's Function & First Passage



$$u(\mathbf{x}) = \int_{\partial\Omega} p(\mathbf{x}, \mathbf{y}) f(\mathbf{y}) d\mathbf{y}.$$

$$u(\mathbf{x}) = \int_{\partial\Omega} \frac{\partial G(\mathbf{x}, \mathbf{y})}{\partial n} f(\mathbf{y}) d\mathbf{y}.$$

$$p(x, y) dy = \mu_{\Omega}^x([y, y + dy])$$

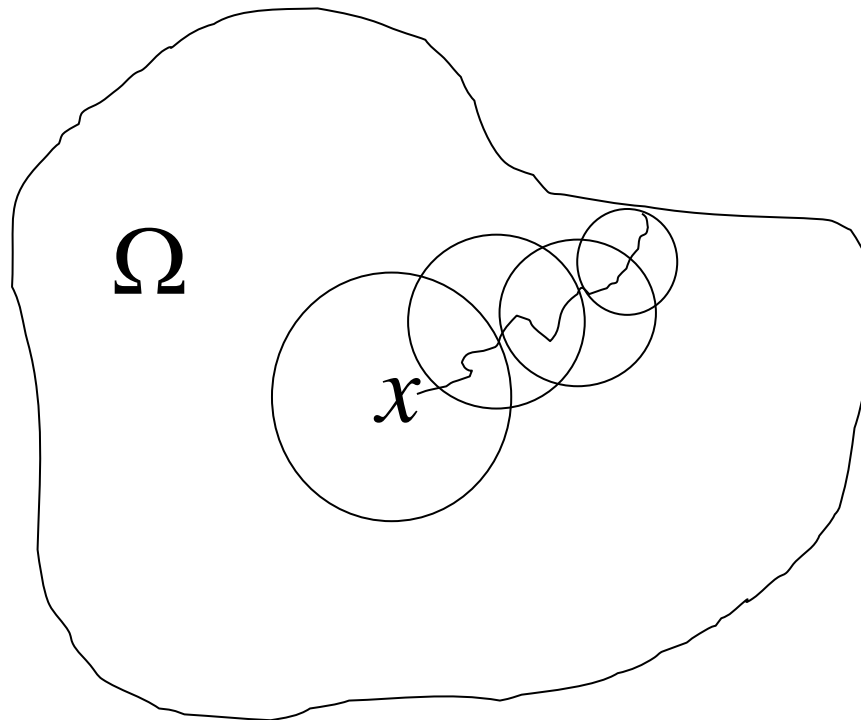
first-passage probability  $\mathbf{p}(\mathbf{x}, \mathbf{y}) d\mathbf{y}$   
of a Brownian particle starting at  $\mathbf{x}$   
hitting the boundary first at  
 $[y, y+dy]$   $\mathbf{y} = X^x(\tau_{\partial\Omega}) \in \partial\Omega$ .

Here  $G(x, y)$  be the Green's function  
which zero Dirichet boundary

$$p(x, y) = \frac{\partial G(x, y)}{\partial n_y}$$

# WOS (Walk on spheres) and sample Brownian Path

- Walk on sphere based on Green's function



# Feynman-Kac formula ( Neumann problem)

$$\begin{cases} (\frac{1}{2}\Delta + q) u = 0, & \text{on } D \\ \frac{\partial u}{\partial n} = \varphi, & \text{on } \partial D \end{cases}$$

- Probabilistic solution (Hsu Pei, 1983)

Feynman-Kac formula :

$$u(x) = \frac{1}{2} E^x \left[ \int_0^\infty e^{q(t)} \varphi(X_t) L(dt) \right]$$

where  $X_t$  is the reflected Brownian motion,  $e^{q(t)} = \exp \left[ \int_0^t q(X_s) ds \right]$  and  $L(dt)$  is the boundary **local time** of standard Brownian Motion.

# Skorohod equation

## Definition

Assume  $D$  is a bounded domain in  $R^d$  with a  $C^2$  boundary. Let  $f(t)$  be a (continuous) path in  $R^d$  with  $f(0) \in \bar{D}$ . A pair  $(\xi_t, L_t)$  is a solution to the Skorohod equation  $S(f; D)$  if the following conditions are satisfied:

- 1  $\xi$  is a path in  $\bar{D}$ ;
- 2  $L(t)$  is a nondecreasing function which increases only when  $\xi \in \partial D$ , namely,

$$L(t) = \int_0^t I_{\partial D}(\xi(s))L(ds); \quad (1)$$

- 3 The Skorohod equation holds:

$$S(f; D): \quad \xi(t) = f(t) - \frac{1}{2} \int_0^t n(\xi(s))L(ds), \quad (2)$$

where  $n(x)$  stands for the outward unit normal vector at  $x \in \partial D$ .

## Skorohod equation

- In above definition , the smoothness constraint on  $D$  can be relaxed to bounded domains with  $C^1$  boundaries, which however will only guarantee the existence of (2). But for a domain  $D$  with a  $C^2$  boundary, the solution will be unique. Obviously,  $(\xi_t, L_t)$  is continuous in the sense that each component is continuous.
- If  $f(t)$  is replaced by the standard Brownian motion (BM)  $B_t$ , the corresponding  $\xi_t$  will be a standard reflecting Brownian motion (RBM)  $X_t$ . Just as the name suggests, a reflecting BM (RBM) behaves like a BM as long as its path remains inside the domain  $D$ , but it will be reflected back inwardly along the normal direction of the boundary when the path attempts to pass through the boundary.

## Boundary local time

### Properties

- (a) It is the unique continuous nondecreasing process that appears in the Skorohod equation (2);
- (b) It measures the amount of time the standard reflecting Brownian motion  $X_t$  spending in a vanishing neighborhood of the boundary within the period  $[0, t]$ . If  $D$  has a  $C^3$  boundary, then

$$L(t) \equiv \lim_{\varepsilon \rightarrow 0} \frac{\int_0^t I_{D_\varepsilon}(X_s) ds}{\varepsilon}, \quad (3)$$

where  $D_\varepsilon$  is a strip region of width  $\varepsilon$  containing  $\partial D$  and  $D_\varepsilon \subset D$ . This limit exists both in  $L^2$  and  $P^x$ -a.s. for any  $x \in \bar{D}$ ;

- (c)  $L(t)$  is a continuous additive functional (CAF) which satisfies the additivity property:  $A_{t+s} = A_s + A_t(\theta_s)$ .

## Boundary local time

An explicit formula

$$L(t) = \sqrt{\frac{\pi}{2}} \int_0^t I_{\partial D}(X_s) \sqrt{ds}, \quad (4)$$

where the the right-hand side of (4) is understood as the limit of

$$\sum_{i=1}^{n-1} \max_{s \in \Delta_i} I_{\partial D}(X_s) \sqrt{|\Delta_i|}, \quad \max_i |\Delta_i| \rightarrow 0, \quad (5)$$

where  $\Delta = \{\Delta_i\}$  is a partition of the interval  $[0, t]$  and each  $\Delta_i$  is an element in  $\Delta$ .

## Neumann problem

We will consider the elliptic PDE in  $R^3$  with a Neumann boundary condition

$$\begin{cases} \left(\frac{\Delta}{2} + q\right) u = 0, \text{ on } D \\ \frac{\partial u}{\partial n} = \phi, \text{ on } \partial D \end{cases}. \quad (6)$$

When the bottom of the spectrum of the operator  $\Delta/2 + q$  is negative a probabilistic solution of (6) is given by

$$u(x) = \frac{1}{2} E^x \left[ \int_0^\infty e_q(t) \phi(X_t) L(dt) \right], \quad (7)$$

where  $X_t$  is a RBM starting at  $x$  and  $e_q(t)$  is the Feynman-Kac functional [?]

$$e_q(t) = \exp \left[ \int_0^t q(X_s) ds \right].$$

- The solution defined in (7) should be understood as a weak solution for the classical PDE (6). The proof of the equivalence of (7) with a classical solution is done by using a martingale formulation [1]. If the weak solution satisfies some smoothness condition [1][2], it can be shown that it is also a classical solution to the Neumann problem.
- Comparing with formula (7), the probabilistic solutions to the Laplace operator with the Dirichlet boundary condition has a very similar form, i.e.  $u(x) = E^x [\phi(X_{\tau_D})]$  where  $\phi$  is the Dirichlet boundary data. In the Dirichlet case, killed Brownian paths were sampled by running random walks until the latter are absorbed on the boundary and  $u(x)$  is evaluated as an average of the Dirichlet values at the first hitting positions on the boundary. For the Neumann condition,  $u(x)$  is also given as a weighted average of the Neumann data at hitting positions of RBM on the boundary, the weight is related to the boundary local time of RBM.

From the definition of the local time in (3), we have the following approximation for small  $\varepsilon$

$$L(t) \approx \frac{\int_0^t I_{D_\varepsilon}(X_s) ds}{\varepsilon}. \quad (8)$$

Plugging (8) into (7), we have

$$u(x) \approx \frac{1}{2\varepsilon} E^x \left[ \int_0^\infty e_q(t) \phi(X_t) \int_t^{t+dt} I_{D_\varepsilon}(X_s) ds \right]. \quad (9)$$

In the present work, as we only consider the Laplace equation where  $q = 0$ , therefore,

$$u(x) \approx \frac{1}{2\varepsilon} E^x \left[ \int_0^\infty \phi(X_t) \int_t^{t+dt} I_{D_\varepsilon}(X_s) ds \right], \quad (10)$$

and we will show how this formula is implemented with the Monte Carlo and WOS methods in next section.

## Walk on Spheres

Random walk on spheres (WOS) method was first proposed by Müller [7], which can solve the Dirichlet problem for the Laplace operator efficiently.

- Idea of WOS: Start from  $x$ , sample  $x_1$  uniformly on a sphere (not touching the boundary) centered at  $x$ , then draw a second sphere (not touching the boundary) centered at  $x_1$ , sample uniformly on the surface of the second sphere, continue until the path hit the boundary.

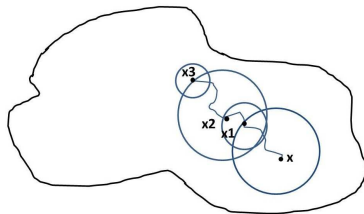


Figure 1: Walk on Spheres method

- Using a jump size (radius of the ball)  $\delta$  on each step for the WOS, we expect to take  $O(1/\delta^2)$  steps for a Brownian path to reach the boundary [6]. To speed up, maximum possible size for each step would allow faster first hitting on the boundary.

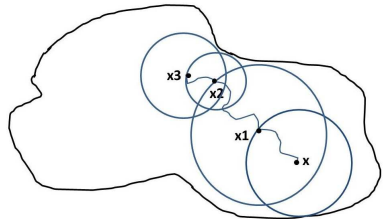


Figure 2: WOS (with a maximal step size for each jump) within the domain

## Simulation of reflecting Brownian paths

- A standard reflecting Brownian motion path can be constructed by reflecting a standard Brownian motion path back into the domain whenever it crosses the boundary. So in principle, the simulation of RBM is reduced to that of BM.
- An  $\varepsilon$ -region is constructed as the termination region in the Dirichlet case. While in Neumann boundary case, the BM  $X_t$  continue moving after the reaching the  $\varepsilon$ -region instead of being absorbed.

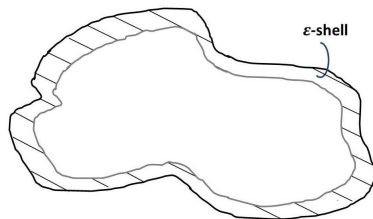


Figure 3: A  $\varepsilon$ -region for a bounded domain in  $R^3$

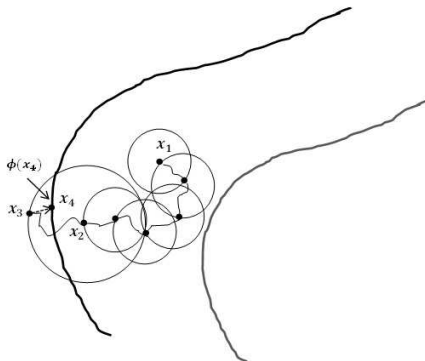


Figure 4: WOS in the  $\varepsilon$ -region.

- Use maximized WOS at each step until BM path hits  $x_1$  in  $\varepsilon$ -region for the first time. Then the radius of sphere is changed to  $\Delta x$ , the path continues until it arrives at  $x_2$  whose distance to  $\partial D$  is smaller or equal to  $\Delta x$ . Then the radius of the ball is enlarged to  $2\Delta x$  so that the path has a chance to run out of the domain at  $x_3$ . If that happens, we pull back  $x_3$  to  $x_4$  which is the closest point to  $x_3$  on the boundary. Record  $\phi(x_4)$ , and continue WOS-sampling the path starting at  $x_4$ .

## Motivation of WOS in $\varepsilon$ -region

The standard Brownian motion can be constructed as the scaling limit of a random walk on a lattice so we can model BM by a random walk with proper scale (see Appendix for details). However, it turns out that the WOS method is the preferred method to simulate BM for our purpose [9].

## One sample path of RBM in cube

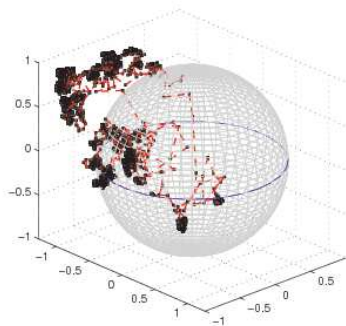


Figure 5: A RBM path with a cube in  $R^3$

## Computing the boundary local time $L(t)$

By (3)

$$L(t) \equiv \lim_{\varepsilon \rightarrow 0} \frac{\int_0^t I_{D_\varepsilon}(X_s) ds}{\varepsilon},$$

which is approximately

$$L(t) \approx \frac{\int_0^t I_{D_\varepsilon}(X_s) ds}{\varepsilon}.$$

Suppose  $x \in D$  is the starting point of a Brownian path, which is simulated by the WOS method. Once the path enters the  $\varepsilon$ -region, the radius of WOS is changed to  $\Delta x$  or  $2\Delta x$ . It is known that the elapsed time  $\Delta t$  for a step of a random walk on average is proportional to the square of the step size, in fact,  $\Delta t = (\Delta x)^2/d, d=3$  when  $\Delta x$  is small (see Appendix), which also applies to WOS moves (See Remark 6 for details).

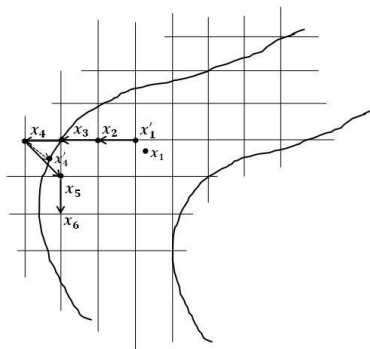


**Figure 6:** Random walks on the  $\varepsilon$ -region. A BM path hits  $x_1 \in M_\varepsilon(D)$  by the WOS method. Replace  $x_1$  by the nearest grid point  $x'_1$ . Then several steps of random walks will make a path as  $x_2 \rightarrow x_3 \rightarrow x_4$ . Since  $x_4 \notin D$ , we push it back along the normal line (dash arrow) to  $x'_4$  then replace it by the closest grid point within domain (solid arrow)  $x_5$ . Here path crosses the boundary at  $x'_4 \in \partial D$ . Then continue the random walk as usual at  $x_6$ .

Therefore,

$$L(dt) = L(t_j - t_{j-1}) \approx \frac{\int_{t_{j-1}}^{t_j} I_{D_\varepsilon}(X_s) ds}{\varepsilon} = (n_{t_j} - n_{t_{j-1}}) \frac{(\Delta x)^2}{3\varepsilon}, \quad (11)$$

where  $n_{t_j} - n_{t_{j-1}}$  is the number of steps that WOS steps remain in the  $\varepsilon$ -region during the time interval  $[t_{j-1}, t_j]$ .

Here notice that by our method within the  $\varepsilon$ -region, the radius of the BM may be  $\Delta x$  or  $2\Delta x$ , which means the corresponding elapsed time of one step for local time will be  $\frac{(\Delta x)^2}{3}$  or  $\frac{(2\Delta x)^2}{3}$ . For the latter, if we absorb the factor 4 into  $nt$ , we will have (11).

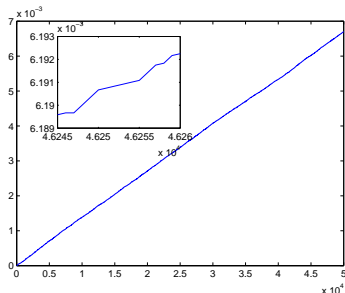


**Figure 7:** Boundary local time increases when the path runs into the region  $M_{\varepsilon}(D)$ . The insert shows the piecewise linear profile of the local time path with flat level regions. The path of  $L(t)$  is a nondecreasing function.

## Probabilistic representation for the Neumann problem

Remember (10)

$$u(x) \approx \frac{1}{2\varepsilon} E^x \left[ \int_0^\infty \phi(X_t) \int_s^{s+dt} I_{D_\varepsilon}(X_s) ds \right]$$

Truncate time frame into  $[0, T]$  and use Monte Carlo method,

$$\tilde{u}(x) = \frac{1}{2\varepsilon} \sum_{i=1}^N \left[ \int_0^T \phi(X_t^i) I_{\partial D}(X_t^i) \int_t^{t+dt} I_{D_\varepsilon}(X_s^i) ds \right], \quad (12)$$

where  $X_t^i, i = 1, \dots, N$  are stochastic processes sampled according to the law of RBM.

Associate the time interval  $[0, T]$  with the number of steps  $NT$  of a sampling path, the integral inside the square bracket in (12) can be transformed into

$$\sum_{j'=1}^{NT} \left( \phi(X_{t_j}^i) I_{\partial D}(X_{t_j}^i) \int_{t_{j-1}}^{t_j} I_{D^c}(X_s^i) ds \right), \quad (13)$$

where  $j'$  stands for the  $j'$ -th step the WOS method has taken, and  $j$  indicates a step for which  $X_{t_j}^i \in \partial D$ .

Replace the occupation time within the local time, (13) becomes

$$\sum_{j'=1}^{NT} \left( \phi(X_{t_j}^i) I_{\partial D}(X_{t_j}^i) (n_{t_j} - n_{t_{j-1}}) \frac{(\Delta x)^2}{3} \right). \quad (14)$$

As a result, an approximation to the PDE solution  $\tilde{u}(x)$

$$\tilde{u}(x) = \frac{1}{2\varepsilon} \sum_{i=1}^N \left[ \sum_{j'=1}^{NT} \left( \phi(X_{t_j}^i) I_{\partial D}(X_{t_j}^i) (n_{t_j} - n_{t_{j-1}}) \frac{(\Delta x)^2}{3} \right) \right]. \quad (15)$$

Theoretically speaking,  $\varepsilon$  should be chosen much larger than  $\Delta x$ . Here, we take  $\varepsilon = k\Delta x$ ,  $k > 1$  is an integer, which will increase as  $\Delta x$  vanishes to zero. Then, (15) reduces to

$$\begin{aligned}\tilde{u}(x) &= \frac{1}{2k\Delta x} \sum_{i=1}^N \left[ \sum_{j=1}^{NT} \left( \phi(X_{t_j}^i) I_{\partial D}(X_{t_j}^i) (n_{t_j} - n_{t_{j-1}}) \frac{(\Delta x)^2}{3} \right) \right] \\ &= \frac{\Delta x}{6k} \sum_{i=1}^N \left[ \sum_{j=1}^{NT} \left( \phi(X_{t_j}^i) I_{\partial D}(X_{t_j}^i) (n_{t_j} - n_{t_{j-1}}) \right) \right],\end{aligned}\tag{16}$$

which is the final numerical algorithm for the Neumann problem.

## Outline of the algorithm

Let  $x$  be any interior point in  $D$  where the solution  $u(x)$  for the Neumann problem is sought. First, we define the  $\varepsilon$ -region  $M_\varepsilon(D)$  near the boundary. For each one of  $N$  RBM paths, the following procedure will be executed until the length of the path reaches a prescribed length given by  $NT \cdot \Delta x$ :

- 1 If  $x \notin M_\varepsilon(D)$ , predict next point of the path by the WOS with a maximum possible radius until the path locates near the boundary within a certain given distance  $\varepsilon$ , say  $\varepsilon = 3\Delta x$  (hit the  $\varepsilon$ -region  $M_\varepsilon(D)$ ). If  $x \in M_\varepsilon(D)$ ,  $l(t_i) = 1$ ; otherwise,  $l(t_i) = 0$ . Here  $l(t)$  is the unit increment of  $L(t)$  at time  $t$ .
- 2 If  $x \in M_\varepsilon(D)$ , use the WOS method with a fixed radius  $\Delta x$  to predict the next location for Brownian path. Then, execute one of the two options:

*Option 1.* If the path happens to hit the domain boundary  $\partial D$  at  $x_{t_i}$ , record  $\phi(x_{t_i})$ .

*Option 2.* If the path passes crosses the domain boundary  $\partial D$ , then pull the path back along the normal to the nearest point on the boundary. Record the Neumann value at the boundary location.

- Due to the independence of the paths simulated with the Monte Carlo method, we can run a large number of paths simultaneously on a computer with many cores in a perfectly parallel manner, and then collect all the data at the end of the simulation to compute the average.

## Preparation

Choose explicit analytical solution to Laplace equation

$$u(x) = \sin 3x \sin 4y e^{5z} + 5.$$

We will test on a circle and line segment within the domain.

### Circle

$$\{(x, y, z)^T = (r \cos \theta_1 \sin \theta_2, r \sin \theta_1 \sin \theta_2, r \cos \theta_2)^T\}$$

with  $r = 0.6$ ,  $\theta_1 = 0 : k \cdot 2\pi/30 : 2\pi$ ,  $\theta_2 = \pi/4$  with  $k = 1, \dots, 15$ .

### Line

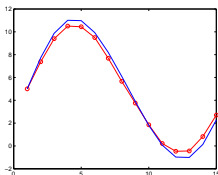
With endpoints  $(0.4, 0.4, 0.6)^T$  and  $(0.1, 0, 0)^T$ , fifteen uniformly spaced points on the line.

### Parameter

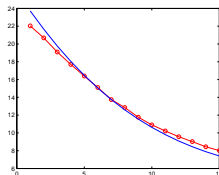
$$N=2e5, \Delta x=0.0005, \varepsilon=3\Delta x$$

## Cube domain

Cube domain of size 2.



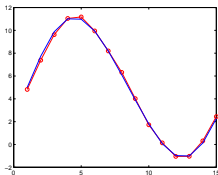
(a)  $\varepsilon = 3\Delta x$ , Err = 9.59%, N-  
P=2.7e4



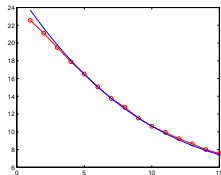
(b)  $\varepsilon = 3\Delta x$ , Err = 11.28%, N-  
P=2.4e4

Figure 8: Cube domain: number of paths  $N = 2e5$ . (Left - circle; right - line) segment.

## Cube domain



(a)  $\varepsilon = 3\Delta x$ , Err = 5.45%, N-P=2.9e4



(b)  $\varepsilon = 3\Delta x$ , Err = 5.47%, N-P=2.5e4

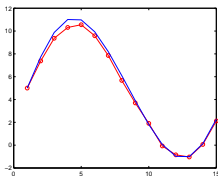
Figure 9: Cube domain: number of paths  $N = 2e5$ . (Left - circle; right - line)

## Cube domain

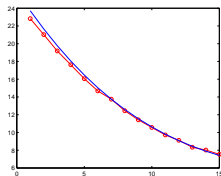
Two choices for the path length parameter  $NP = 2.7e4$  and  $NP = 2.9e4$  for the circle ( $NP = 2.4e4$  and  $NP = 2.5e4$  for the line segment) are compared to gauge the convergence of the numerical formula in terms of the path truncation. Figures 8 and 9 shows the solution and the relative errors in both cases, which indicates that  $NP = 2.9e4$  and  $NP = 2.5e4$  will be sufficient to give an error around 5% for circle and line segment respectively as shown in Fig. 9.

## Spherical domain

The unit ball is centered at the origin.



(a)  $\varepsilon = 3\Delta x$ , Err = 5.93%,  $N = 5e4$



(b)  $\varepsilon = 3\Delta x$ , Err = 5.83%,  $N = 4.5e4$

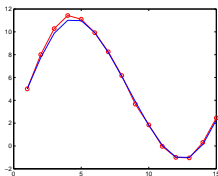
**Figure 10:** Spherical domain: number of paths  $N = 2e5$ . (Left) Solution on the circle; (right) solution on a line segment.

## Spherical domain

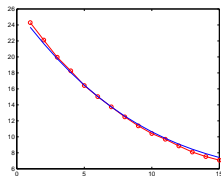
Similar numerical results are obtained as in the case of the cube domain. Here, the reflected points of Brownian path are the intersection of the normal and the domain. Though both Figure 10(a) and (b) shows little deviation in the beginning, the overall approximation are within an acceptable relative error less than 6%.

## Ellipsoid domain

The ellipse with axis lengths (3, 2, 1) is centered at the origin.



(a)  $\varepsilon = 3\Delta x$ , Err = 5.12%, N-P=6.3e4



(b)  $\varepsilon = 3\Delta x$ , Err = 5.45%, N-P=5.3e4

**Figure 11:** Ellipsoid domain: number of paths  $N = 2e5$ . (Left) Solution on the circle; (right) solution on a line segment.

## 3d random walks converge to brownian motion

If the random walk on a lattice as in Fig. 11 is to converge to a continuous BM, a relationship between  $\Delta t$  and  $\Delta x$  in  $R^3$  will be needed and is shown to be

$$\Delta t = \frac{(\Delta x)^2}{3}. \quad (17)$$

The following is a proof for this result (See [?] for reference). The density function of standard BM satisfies the following PDE [?]

$$\frac{\partial p}{\partial t} = \frac{1}{2} \Delta_x p(t, x, y). \quad (18)$$

By using a central difference scheme and changing  $p$  to  $v$ , equation (18) becomes

$$\frac{v_{i,j,k}^{n+1} - v_{i,j,k}^n}{\Delta t} = \frac{1}{2} \frac{v_{i+1,j,k}^n + v_{i-1,j,k}^n + v_{i,j+1,k}^n + v_{i,j-1,k}^n + v_{i,j,k+1}^n + v_{i,j,k-1}^n - 6v_{i,j,k}^n}{(\Delta x)^2}. \quad (19)$$

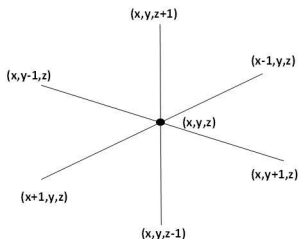


Figure 12: Central difference scheme in  $R^3$

Reorganizing and letting  $\lambda = \Delta t / (2(\Delta x)^2)$ , we have

$$v_{i,j,k}^{n+1} = \lambda v_{i+1,j,k}^n + \lambda v_{i-1,j,k}^n + \lambda v_{i,j+1,k}^n + \lambda v_{i,j-1,k}^n + \lambda v_{i,j,k+1}^n + \lambda v_{i,j,k-1}^n + (1 - 6\lambda) v_{i,j,k}^n, \quad (20)$$

By setting  $\lambda = \frac{1}{6}$ , we have

$$v_{i,j,k}^{n+1} = \frac{1}{6} v_{i+1,j,k}^n + \frac{1}{6} v_{i-1,j,k}^n + \frac{1}{6} v_{i,j+1,k}^n + \frac{1}{6} v_{i,j-1,k}^n + \frac{1}{6} v_{i,j,k+1}^n + \frac{1}{6} v_{i,j,k-1}^n. \quad (21)$$

For the initial condition  $\phi$ , we have

$$v_{i,j,k}^{n+1} = \sum_{i',j',k'} C_{i',j',k'} \phi \left( \sum_{l=1}^n \vec{\eta}_l \right) \quad (22)$$

where

$$\vec{\eta}_l = \begin{cases} (-h, 0, 0)^T, & \text{prob} = \frac{1}{6} \\ (h, 0, 0)^T, & \text{prob} = \frac{1}{6} \\ (0, h, 0)^T, & \text{prob} = \frac{1}{6} \\ (0, -h, 0)^T, & \text{prob} = \frac{1}{6} \\ (0, 0, h)^T, & \text{prob} = \frac{1}{6} \\ (0, 0, -h)^T, & \text{prob} = \frac{1}{6} \end{cases}, \quad (23)$$

and

$$\sum_{l=1}^n \vec{\eta}_l = \begin{pmatrix} -n + 2i' + i \\ -n + 2j' + j \\ -n + 2k' + k \end{pmatrix} h. \quad (24)$$

Let  $\vec{\eta}_l = (x_l, y_l, z_l)^T$ , then

$$x_l = \begin{cases} -h, & \text{prob} = \frac{1}{6} \\ h, & \text{prob} = \frac{1}{6}, \\ 0, & \text{prob} = \frac{2}{3} \end{cases}, \quad (25)$$

for each  $l$ . We known that  $y_l, z_l$  have the same distribution as  $x_l$ .

Notice that the covariance between any two of  $x_l, y_l, z_l$  is zero, i.e.  $E(x_l y_l) = 0$ ,  $E(y_l z_l) = 0$  and  $E(x_l z_l) = 0$ . So  $E(\sum_{i=1}^n x_l \sum_{i=1}^n y_l) = 0$ ,  $E(\sum_{i=1}^n y_l \sum_{i=1}^n z_l) = 0$  and  $E(\sum_{i=1}^n x_l \sum_{i=1}^n z_l) = 0$ . According to the central limit theorem, we have

$$\sum_{i=1}^n x_l \stackrel{D}{=} N\left(0, \frac{nh^2}{3}\right) \text{ as } n \rightarrow \infty. \quad (26)$$

The same assertion holds for  $\sum_{i=1}^n y_l$  and  $\sum_{i=1}^n z_l$ . Since  $\lambda = \frac{\Delta t}{2(\Delta x)^2} = \frac{1}{6}$ , then  $h^2 = 3k$  and hence  $\frac{nh^2}{3} = nk = t$ . Therefore  $\sum_{i=1}^n x_l \sim N(0, t)$  as  $n \rightarrow \infty$ . So are  $\sum_{i=1}^n y_l$  and  $\sum_{i=1}^n z_l$ .

Recall that the covariance between any pair of  $\sum_{i=1}^n x_l, \sum_{i=1}^n y_l$ , and  $\sum_{i=1}^n z_l$  is zero, that  $\sum_{i=1}^n x_l, \sum_{i=1}^n y_l$  and  $\sum_{i=1}^n z_l$  are independent normal random variables.

Hence,

$$C_{i',j',k',n} = P \left\{ \sum_{l=1}^n \vec{\eta}_l = \begin{pmatrix} -n + 2i' + i \\ -n + 2j' + j \\ -n + 2k' + k \end{pmatrix} h = \begin{pmatrix} \sum_{i=1}^n x_l \\ \sum_{i=1}^n y_l \\ \sum_{i=1}^n z_l \end{pmatrix} \right\} \xrightarrow{D} \frac{1}{(2\pi t)^{3/2}} e^{-\frac{\|\vec{x} - \vec{x}_0\|^2}{2t}}, \quad (27)$$

and

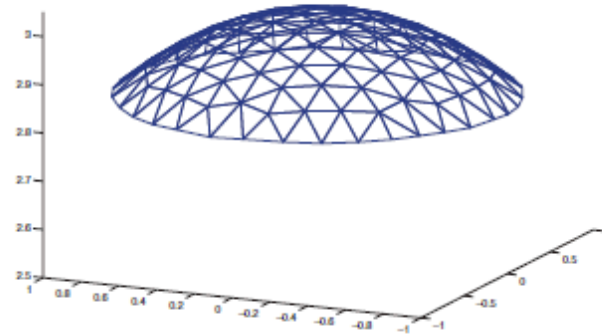
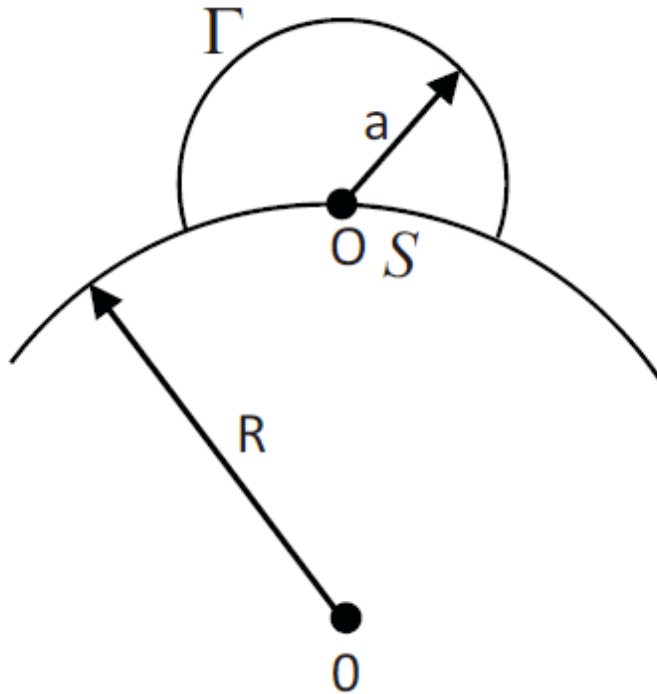
$$v_{i,j,k}^{n+1} = \sum_{i',j',k'} C_{i',j',k',n} \phi \left( \sum_{l=1}^n \vec{\eta}_l \right) \rightarrow \iiint_{R^3} \frac{1}{(2\pi t)^{3/2}} e^{-\frac{\|\vec{x} - \vec{x}_0\|^2}{2t}} \phi(\vec{x}) d\vec{x}, \quad (28)$$

which coincides with the density function of the 3-d standard BM.

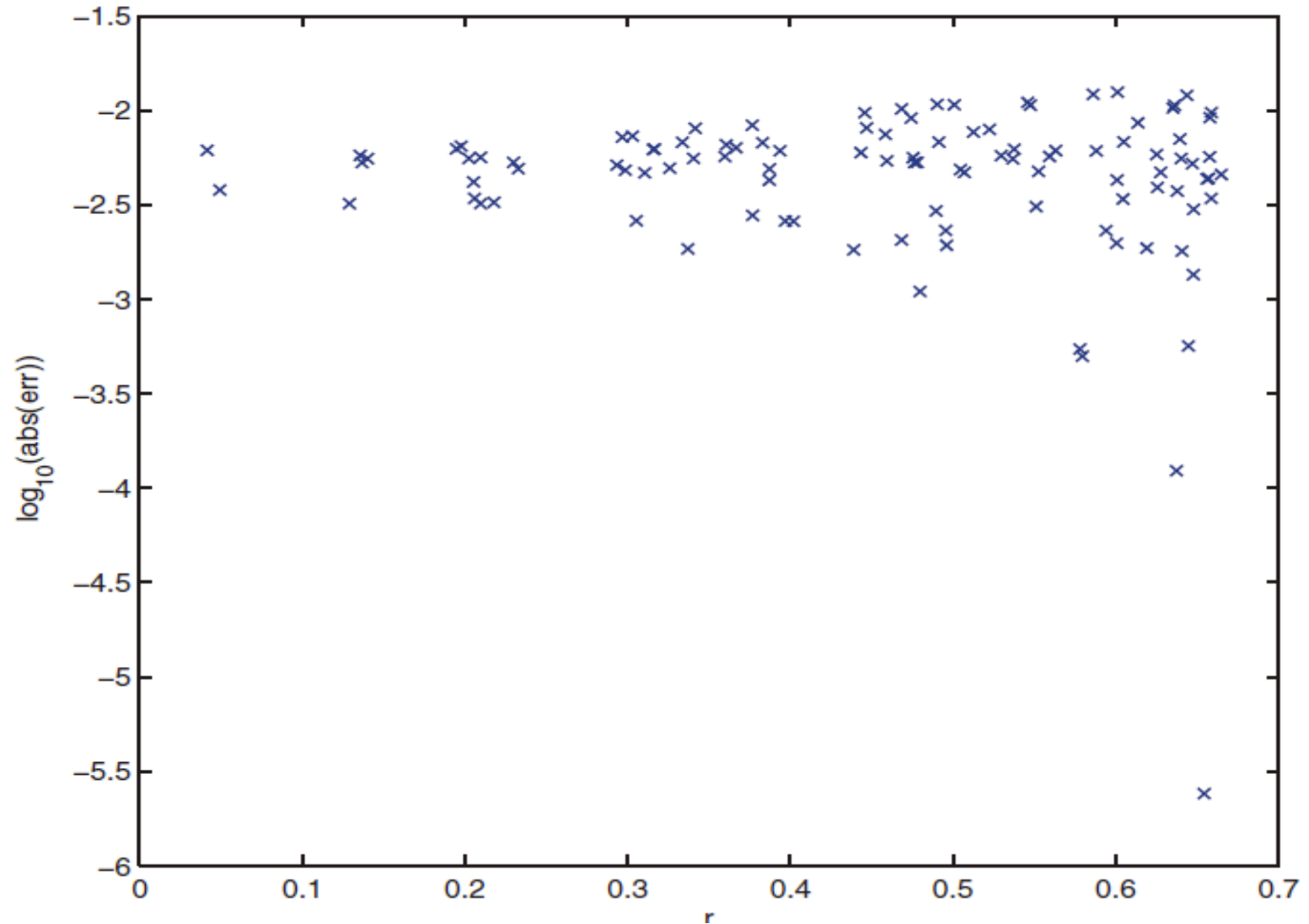
In conclusion, when  $\frac{\Delta t}{2(\Delta x)^2} = \frac{1}{6}$ , i.e.  $\Delta t = \frac{(\Delta x)^2}{3}$  or  $\sqrt{dt} = \frac{dx}{\sqrt{3}}$ , the central difference scheme converges to the standard BM in 3- $d$ . Generally, the result can be extended to  $d$ -dimensional Euclidean space and the result will be  $\Delta t = \frac{(\Delta x)^2}{d}$ .

# Scaling performance of DD BIE

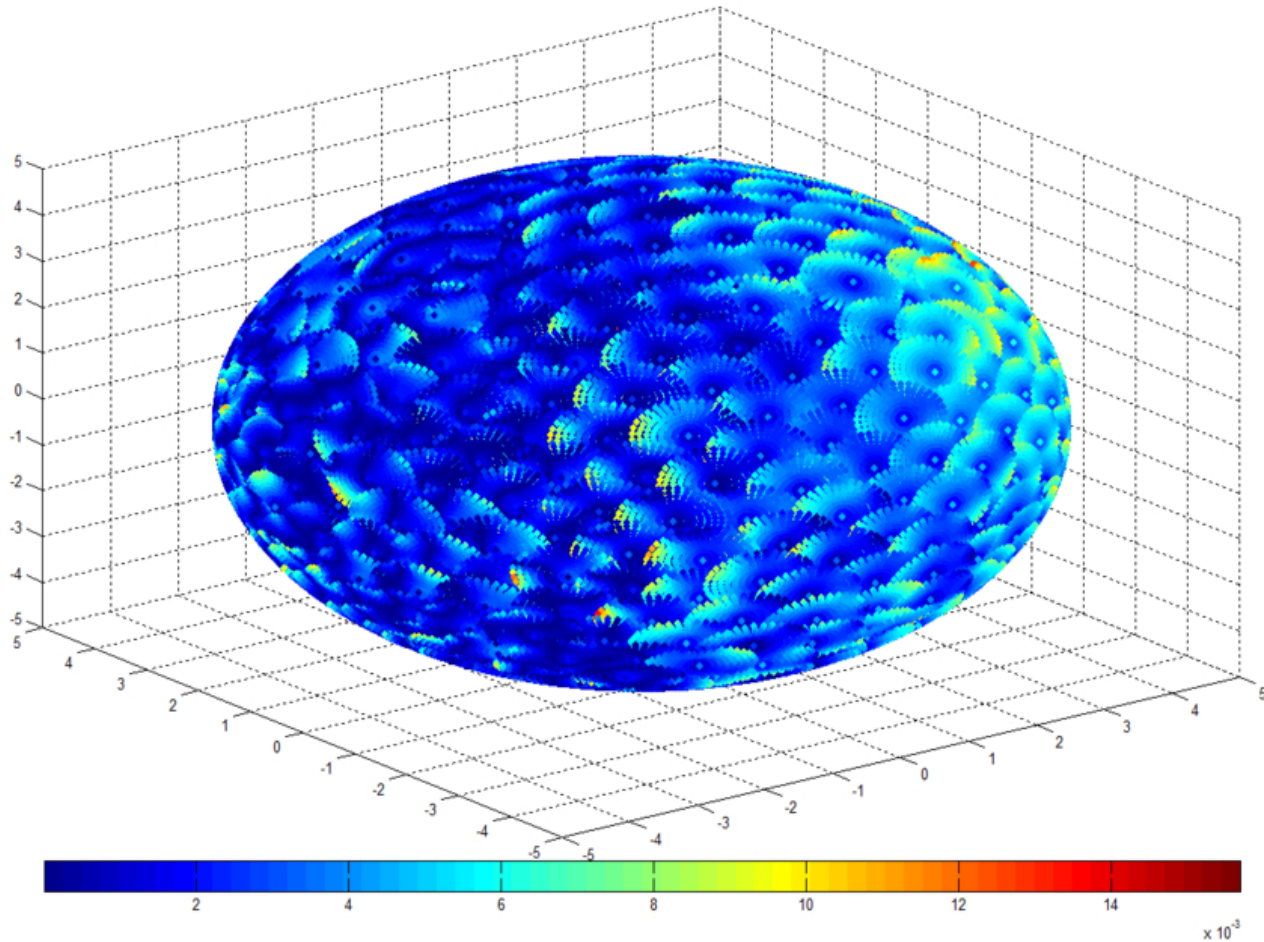
# Test Case 1—Accuracy of a curve patch



# Test Case 1-Accuracy of a curved patch



# Test Case 2—a large sphere

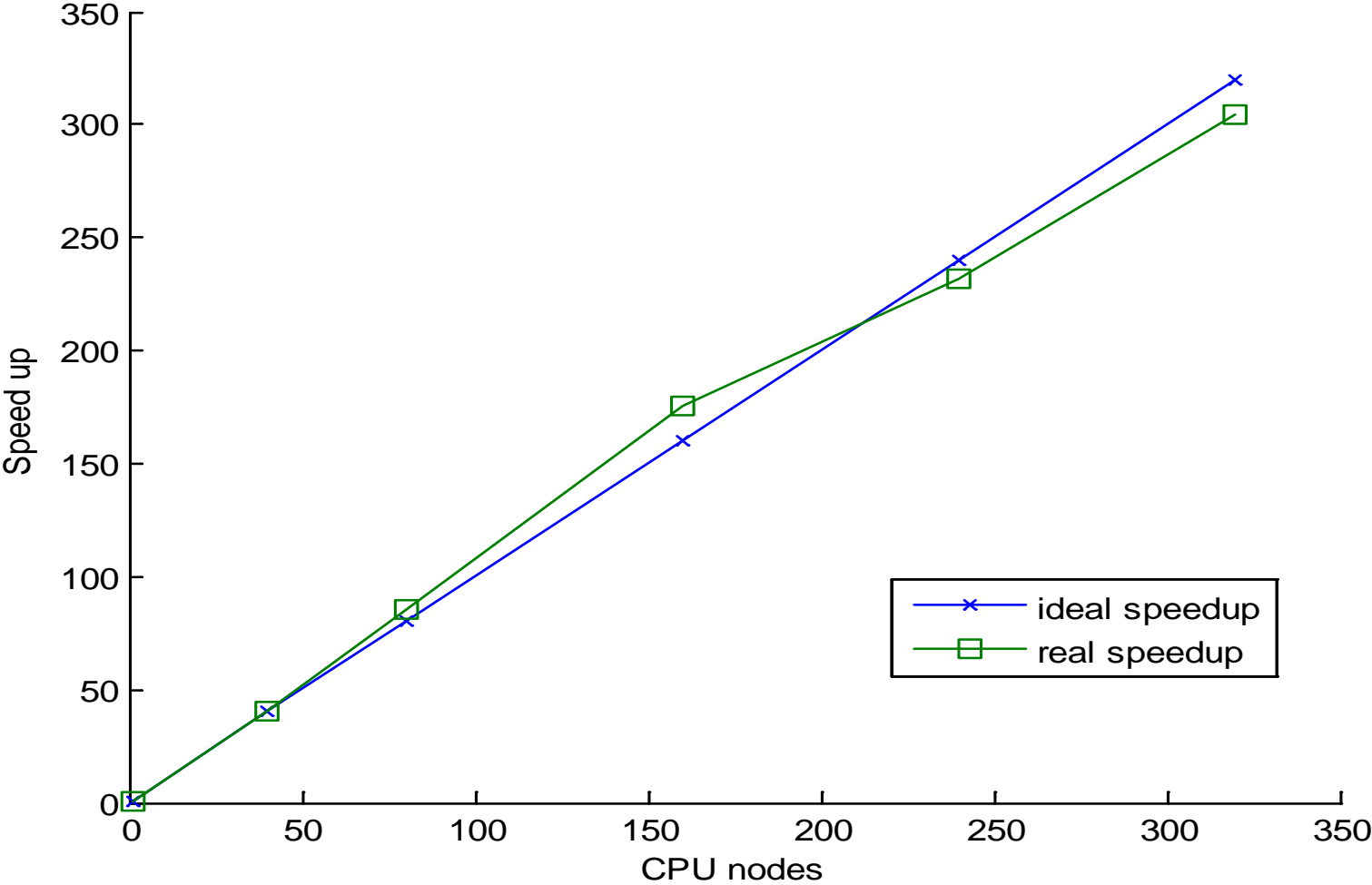


# Test Case 2—a large sphere

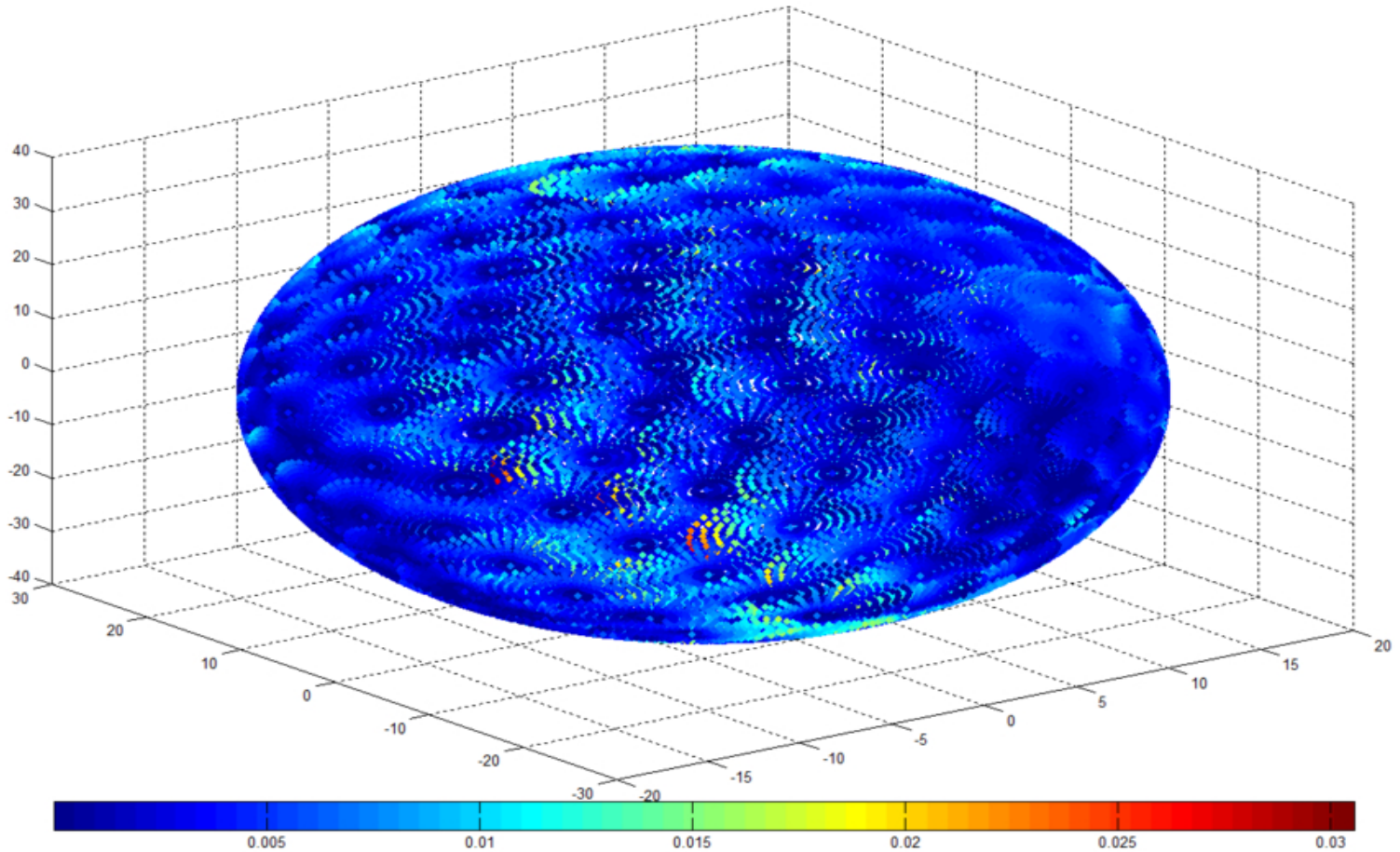
Task load	#unknowns	# Computational node	#cpu cores	Wall time(s)	Normalized Speedup (cpu time of 16 cores as 1)	r<0.7a Max error (%)
1x	432	1	16	222.00	1.0	
40x	1.73x10 <sup>4</sup>	40	640	222.52	40.0	1.35
80x	3.46x10 <sup>4</sup>	80	1280	207.19	85.9	1.35
160x	6.91x10 <sup>5</sup>	160	2560	203.34	175.1	1.46
240x	1.04 x10 <sup>5</sup>	240	3840	229.89	232.3	1.46
320x	1.38 x10 <sup>5</sup>	320	<b>5120</b>	234.18	304.1	1.46

# Test Case 3—a large sphere

The Scalability of Sphere case



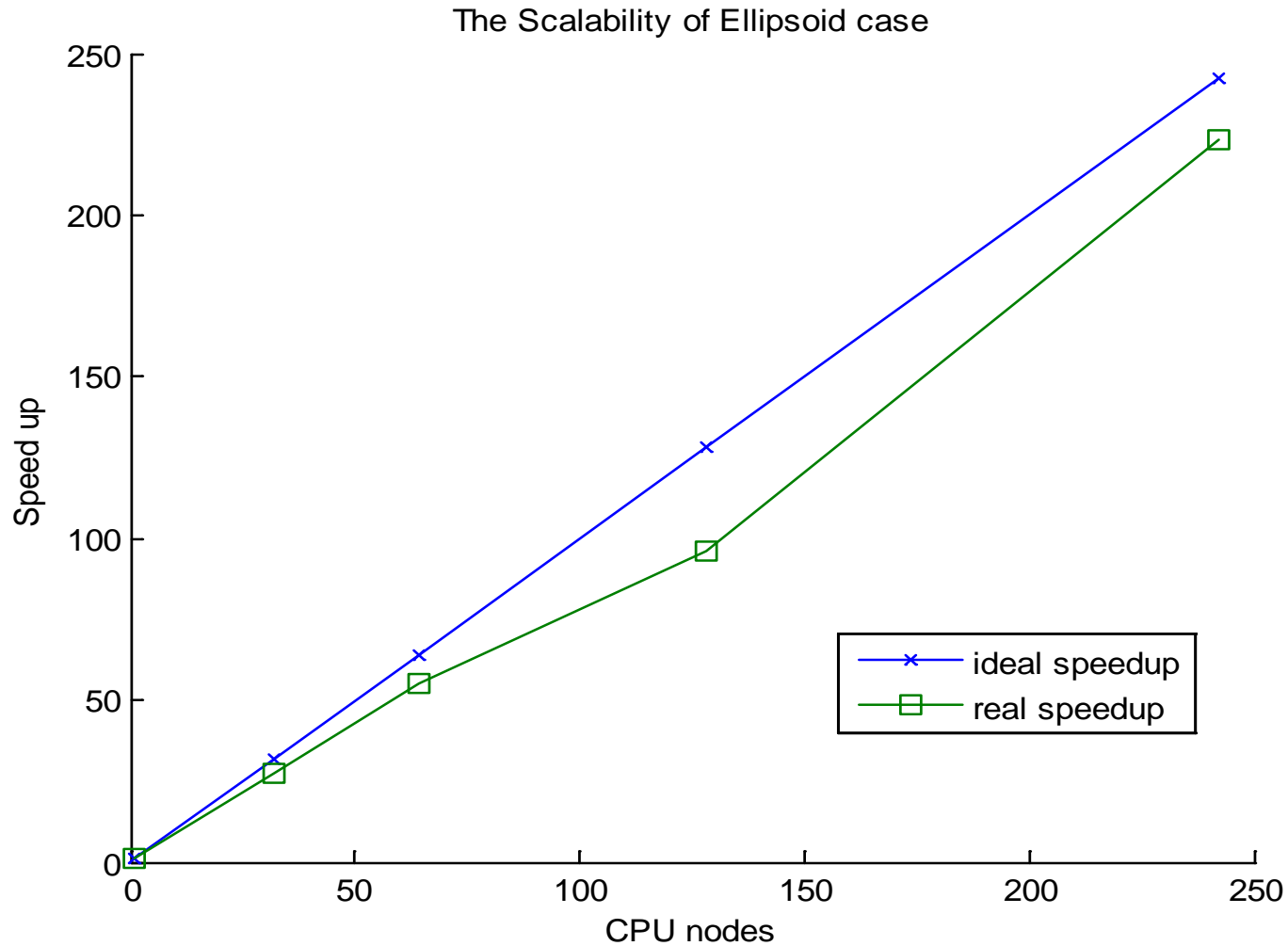
# Test Case 3—a large ellipsoid



# Test Case 4—a large ellipsoid

Task load	#unknowns	#Computational node	#cpu cores	Wall time(s)	Normalized Speedup (cpu time of 16 cores as 1)	r<0.7a Max error (%)
1x	432	1	16	1069.94	1.0	
32x	1.38x10 <sup>4</sup>	32	512	1248.94	27.5	2.35
64x	2.74x10 <sup>4</sup>	64	1024	1239.91	55.4	2.35
128x	5.53x10 <sup>5</sup>	128	2048	1426.46	96.2	2.35
242x	1.05x10 <sup>5</sup>	242	<b>3872</b>	1164.05	223.0	3.06

# Test Case 3—a large ellipsoid



# Other issues

- Treatment of inhomogeneous term

$$(-\Delta + k^2)G = g$$

Compact support  $\sup(g), G \rightarrow 0, |x| \rightarrow \infty$

Use FFT, we can obtain  $G$  in  $O(N \log N)$

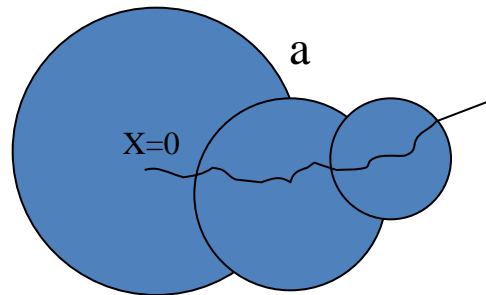
$$u \rightarrow u - G$$

$$\phi|_{\partial\Omega} \rightarrow (\phi - G)|_{\partial\Omega}$$

- Treatment of lower order term  $k \neq 0$

$$u(x) = E^x[\phi(X_{\tau_\Omega}) \exp\{-k^2 \tau_\Omega\}]$$

$$u(0) = \frac{1}{I_0(ka)} \frac{1}{2\pi} \int_0^{2\pi} u(a, \theta) d\theta$$



# Projection Methods for N-S

$$\begin{aligned} \partial_t u + u \cdot \nabla u - \nu \Delta u + \nabla p &= f(x, t), \\ \nabla \cdot u &= 0. \end{aligned}$$

Step 1: Compute an intermediate velocity field  $\tilde{u}^{k+1}$  by

$$(28) \quad \frac{1}{\Delta t} (\tilde{u}^{k+1} - u^k) - \nu \Delta \tilde{u}^{k+1} + u^k \cdot \nabla u^k = f(t^{k+1}), \quad \text{Helmholtz solver w. Dirichlet BC}$$

$$\tilde{u}^{k+1}|_{\partial\Omega} = w.$$

Step 2: Enforcement of incompressibility condition using the pressure variable  $p^{k+1}$

$$(29) \quad \frac{1}{\Delta t} (u^{k+1} - \tilde{u}^{k+1}) + \nabla p^{k+1} = 0, \quad \nabla \cdot u^{k+1} = 0,$$

$$u^{k+1} \cdot n|_{\partial\Omega} = w \cdot n,$$

which gives a Poisson equation for  $p$  with a Neumann boundary conditions as follows

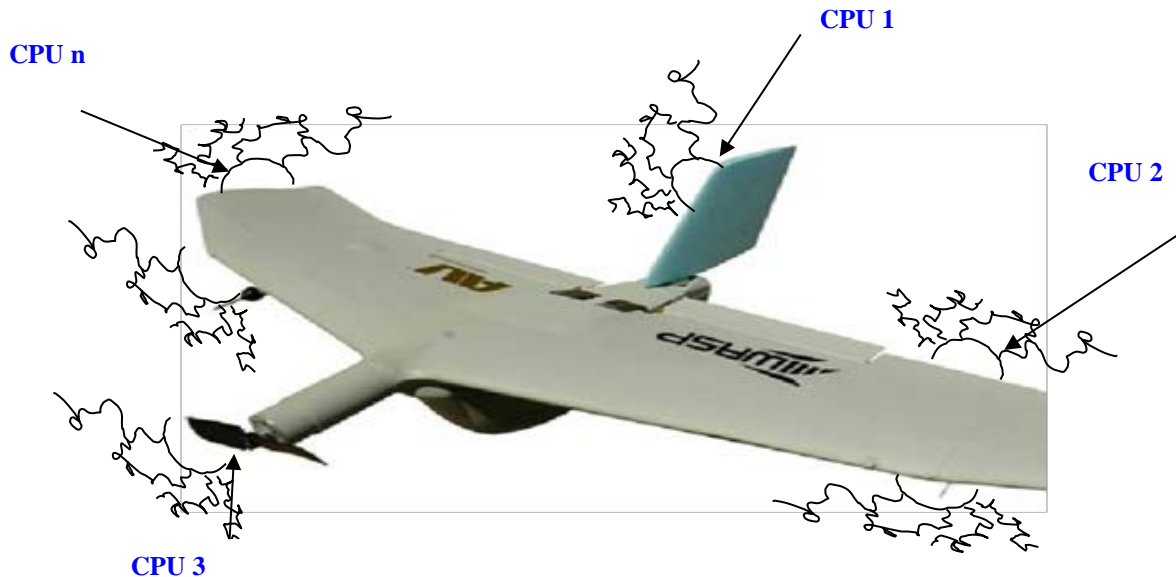
$$(30) \quad \Delta p^{k+1} = g, \quad \frac{\partial p^{k+1}}{\partial n}|_{\partial\Omega} = 0.$$

Poisson Solver  
w. Neumann BC

# A parallel algorithm in 3-D

$$(-\Delta + k^2)u(x) = g$$

$$u|_{\partial\Omega} = \phi(z), z \in \partial\Omega$$



BIE-WOS on each half sphere will produce independently

$$\frac{\partial u}{\partial n} \Big|_{\partial\Omega}$$

# Comparison with FE/FD/IE for potential problems in 3-D

## BIE-WOS



### Pros:

- No large linear system to invert
- Only local IE to solve
- Complete parallelism
- No FE/FV meshes needed

### Cons:

- MC sampling accuracy
- Laplace or PB eqs only

## Grid based methods

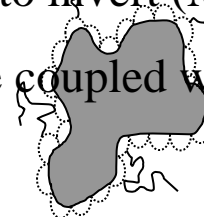
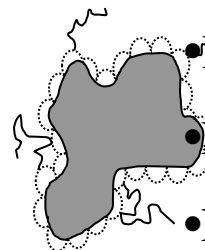
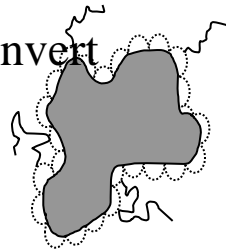


### Pros:

- High order accuracy
- General PDEs

### Cons:

- Large system to invert (Multigrid or Krylov space coupled with FMM  $O(N)$ )
- Per iteration
- Parallel not easy for MG and FMM



## • Publication

1. C.H. Yan, W. Cai, X. Zeng, A parallel method for solving Laplace equations with Dirichlet data using local boundary integral equations and random walks. **SIAM J. Scientific computing** (2013), vol. 35, No. 4, pp. B868-B889.
2. Yijing Zhou, Wei Cai, Elton Hsu, Computation of Local Time of Reflecting Brownian Motion and Probabilistic Representation of the Neumann Problem, submitted to CiCP, 2015.

# Summary and open issues

- DD BIE with Feynman-Kac formula is ideal for scalable parallel computing
- Open issues
  - reduction of cost for each local patch
  - fast calculation of distance to general boundaries
  - complex domain in biomolecules
  - transmission problems in PB/P equations

# Acknowledgement

- Dirichlet data: Yan Chanhao, Zeng Xuan, Fudan
- Neumann data: Zhou yijing, Ph.D. student, UNCC, Pei Hsu, NWU
- Parallel scaling performance: Yan Chanhao, Fudan

Research Supported by NIH and NSF